Modeling of Electrical Transients in the Semiconductor/Electrolyte Cell for Photogeneration of Charge Carriers in the Bulk†

K. Schwarzburg‡ and F. Willig*,‡

Fritz-Haber-Institut der MPG, Physical Chemistry, Faradayweg 4-6, 14195 Berlin, Germany

Received: September 6, 1996; In Final Form: December 29, 1996⊗

Firstly, the time-dependent diffusion of minority carriers occurring in picosecond−nanosecond windows and, secondly, recombination losses occurring in microsecond−millisecond windows were modeled with differential equations. The latter were incorporated as properties of active sources that were embedded into an equivalent circuit that had been tested previously. The shape and magnitude of the electrical response created by illuminating the photo-electrochemical cell were measured in the external circuit and were fitted quantitatively to the minority carrier diffusion model and to the recombination loss model operative in the respective time windows.

Introduction

The interface between a solution containing redox ions and a semiconductor facilitates the exchange of charge between the two different media. This is of fundamental importance when this interface is part of a photovoltaic device.[1] However, molecular groups at the surface of the semiconductor can also react with solvent molecules, and thereby the chemical composition of the interface is changed. The thus formed (photo)-corrosion layer eventually hinders the exchange of charge across the interface. The latter effect has prevented until now the practical application of semiconductor/electrolyte cells as photovoltaic devices.

Nevertheless, the semiconductor/electrolyte interface offers definite advantages over solid state devices for investigating the important relationship between the speed of the interfacial discharge reaction and the occurrence of recombination losses in the semiconductor electrode at a given light intensity. The advantages of the liquid contact are the easy preparation of the interface and the possibility of varying the concentration and energetic position of electronic states, i.e. redox ions in the solution, that participate in the interfacial charge transfer processes. For obtaining meaningful and reproducible results, such measurements have to be restricted to a certain period of time after the preparation of a fresh interface, when corrosion effects are still negligible.

In the field of photo-electrochemistry the electrical response of the system is generally measured to probe the flow of charges in the system under different experimental conditions. In the simplest approach the RC-controlled time-dependent behavior of the semiconductor/electrolyte system can be modeled with an equivalent circuit, where the spatial separation of photogenerated electron−hole pairs is represented by two capacitors, the first for the depletion layer in the semiconductor and the second for the Helmholtz layer at the solution side of the interface. Several authors[2−8] have confirmed the usefulness of this approximation for modeling the RC-controlled time-dependent behavior of the system. However, the time dependence of the electrical response caused by the most important physical processes occurring in this system, e.g. diffusion of the minority carriers toward the depletion layer and recombination of electron−hole pairs across the depletion layer, cannot be modeled in the behavior of an equivalent circuit that consists only of passive circuit elements. An important improvement in modeling the latter processes was obtained by describing the kinetic processes with differential equations and incorporating those properties into active current sources that were embedded into the equivalent circuit.[5,8,9] Hitherto the latter concept had been tested mainly in picosecond−nanosecond (ps−ns) windows by fitting corresponding models to photogenerated electrical transients. However, when neat single crystals, e.g. GaAs or Si, are applied as electrodes, the important recombination processes should be much slower and should occur in microsecond−millisecond (μs−ms) windows.

In this paper experimental electrical transients are presented that were generated via light absorption in a single crystal n-Si electrode. The signals were measured over a wide range of time scales, i.e. in ps−ns windows and also in μs−ms windows. Applying the above kinetic approach the experimental transients were modeled in both the ps−ns windows and μs−ms windows. It is shown that modeling the kinetic processes in the system with the above approach succeeds in fitting the experimental transient signals. This provides direct insight into the interplay between the speed of the interfacial reaction, band bending in the semiconductor, and the occurrence of recombination losses, in particular in the important μs−ms windows.

Experimental Section

For ps−ns photocurrent measurements a synchronously pumped dye laser with a cavity dumper (Spectra Physics) was used as a light source (10 ps fwhmh, 10 nJ pulse, at $\lambda = 590$ nm). For data acquisition the photocurrent was amplified (two cascaded broad-band amplifiers B&H, 8 GHz bandwidth) by 40 dB and the signal was measured with a Tektronix sampling oscilloscope (Tektronix 7904 with 7S11 and 7T11 plug-ins). The oscilloscope was controlled and read out by a PC. The signal could be averaged at a rate of 100 curves/s. For achieving a high time resolution of 100 ps, the sample was mounted on a 50 Ω matched microstrip and an electrode surface of only 1 mm diameter was used. The setup has been described in more detail in refs 5 and 8.

Light pulses with a rectangular time profile (ms-measurements) were generated with a modulated laser diode ($\lambda = 655$ nm, 3 mW, 100 MHz modulation BW). Leakage light imping-

† In memory of the late Heinz Gerischer, who we owe the introduction to this field.

‡ Present address: Hahn-Meitner-Institut, Physical Chemistry, Glienickerstr. 100, 14109 Berlin, Germany.

⊗ Abstract published in *Advance ACS Abstracts,* March 15, 1997.

S1089-5647(96)02726-5 CCC: $14.00

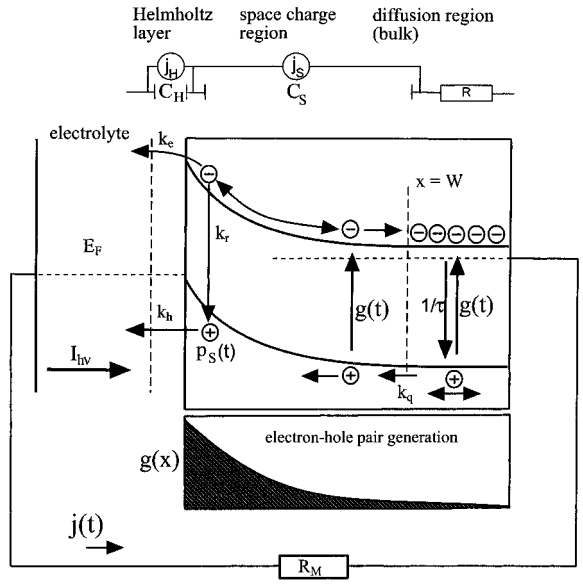

Figure 1. Pictorial representation of the processes occurring in a photoelectrochemical cell under illumination. The equivalent circuit is shown at the top.

ing during the dark phase of the signal was blocked with an additional mechanical shutter that was synchronized to the laser diode modulation. The electrochemical cell was connected to a home-built potentiostat (1 MHz bandwidth), and the current output was averaged and recorded with a digital oscilloscope (Lecroy 7200). To make the measurements as reproducible as possible, the cell was automatically disconnected from the potentiostat between measurements. Samples were mounted on a glass capillary and sealed with silicon glue (Wacker). The electrode surface was 2 mm in diameter. A Pt counter electrode was used. The electrolyte was stirred and bubbled with nitrogen. Ohmic contacts were prepared with an InGa eutectic and silver paste. All the time-resolved measurements, in ps−ns and μs−ms windows, were performed with a two-electrode arrangement.

(100)-oriented n-Si single crystals with donor density of $\sim 10^{15}$ cm^{-3} (3−6 Ω cm^{-1}) were used as electrodes. Each electrode was etched with 49% HF(aq) and rinsed with MeOH. 1,1′-Dimethylferrocene (Me_2Fc)/1,1′-dimethylferrocenium tetrafluoroborate was the redox couple and 0.5 M LiCl the supporting electrolyte in MeOH. All chemicals were purchased reagent grade quality and were further dried and purified by standard methods.

Model signals were generated by solving the rate and circuit equations with the stiff ordinary differential equation solver LSODE.[10] The ode solver was coupled with a nonlinear least-squares fitting routine.[11]

Model for the Photogenerated Electrical Transient at Low Light Intensity

The most important processes involving photogenerated electron−hole pairs in the photo-electrochemical cell with an n-type semiconductor electrode are depicted in Figure 1. With the light pulse impinging from the left-hand side electron−hole pairs are created in the absorption layer of the semiconductor with rate $g(t,x)$. In the general case, a space charge region of width W (several 100−1000 Å) is established in the dark at the semiconductor/electrolyte interface, and the latter supplies an electric field for electron−hole pair separation. At the interface holes in the valence band can take up electrons from the reduced redox ions in solution with rate constant k_h. Electrons in the conduction band can be transferred to oxidized redox ions with rate constant k_e. The electrical circuit is closed via transport of electrical charge through the solution and through the resistors, capacitors, and leads forming the external loop. The current flow through the semiconductor/electrolyte interface is called "Faradaic current" when electrical charge is transferred across the Helmholtz layer at the surface of the semiconductor electrode. It is called "charging current" when only the charge density is changed at the surface of the semiconductor electrode without charge transfer across the Helmholtz layer. As will be shown here, the electrical transients measured at an external resistor can have identical shape and magnitude for these two fundamentally different cases. The so-called small signal approximation where only the transport of minority carriers is considered in the potential prepared in the dark can fail even at very low light intensity when electron transfer across the Helmholtz layer is very slow. It fails again even for a fast interfacial reaction when the photon flux is high. The simultaneous exact treatment of all the different processes in one unified model is rather demanding. It would involve light absorption, Poisson's equation that determines the spatial dependence of the field in the space charge layer, drift-diffusion equations for the transport of electrons and holes in the semiconductor[12] and of charge through the electrolyte,[13] recombination of electrons and holes in the bulk, in the depletion layer, and via the electrolyte, electron transfer across the Helmholtz layer at the surface of the semiconductor,[14] and finally transport of charges through the external circuit and through the Helmholtz layer at the counter electrode.

In this paper it is explored whether the following grossly simplified model is sufficient for understanding salient features of electrical transients in the semiconductor/electrolyte cell generated via photogeneration of charge carriers in the bulk. The important simplification in the model is the definition of differential equations for describing electron−hole pair transport and kinetics without solving explicitly for the spatial dependence. These differential equations determine the properties of the active current sources that shunt the capacitive elements, where the latter represent the spatial separation of electrons and holes. There are also some additional resistors in the equivalent circuit of the passive elements, illustrated at the top of Figure 1. The capacitive properties of the space charge region and of the Helmholtz layer are represented by capacitors C_S and C_H, respectively. Time-dependent transport of charge carriers across the depletion layer region and across the Helmholtz layer is modeled by the current source $j_S(t)$ and $j_H(t)$, respectively. The equivalent circuit part of the model is shown at the top of Figure 1. The series resistor R accounts for ohmic losses occurring in the bulk of the semiconductor, at the back contact, and in the electrolyte. Modeling spatial electron−hole pair separation in the space charge regions remains valid only as long as the change in voltage under illumination is small enough such that the charge distribution remains close to the situation that prevails in the dark. The general voltage response $U_M(t)$ in this model system, measured at the external resistor R_M, can be expressed as a convolution of the internal current sources, j_S, j_H, with the RC response of the circuit:[5]

$$U_M(t) = \frac{R_M}{(R_M + R)C_S}\int_0^t e^{-(t-t')/\tau}\left(j_S(t') + \frac{C_S}{C_H} j_H(t')\right) dt'$$

$$\frac{1}{\tau} = \left(\frac{1}{C_S} + \frac{1}{C_H}\right)\frac{1}{R_M + R} \qquad (1)$$

For a low- to moderately-doped semiconductor, the space charge capacitor is several orders of magnitude smaller than the capacitor that stands for the Helmholtz layer. The opposite

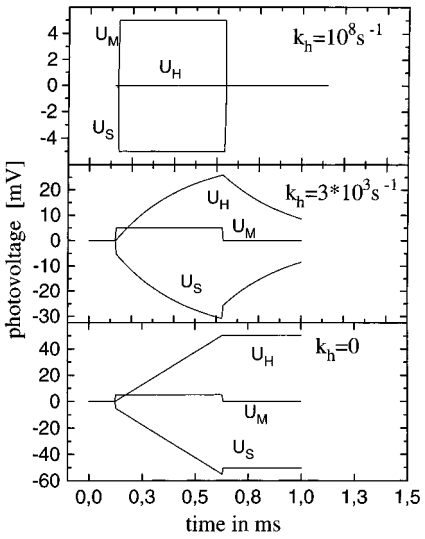

Figure 2. Simulation of the transient photocurrent response to a light pulse with a rectangular time profile (according to eqs 1 and 2a−c). Simulation parameters: $C_S = 100$ pF, $C_H = 10$ nF, $R_M = 50$ Ω, $R = 0$ Ω.

holds true for the widths of the layers. Therefore, the voltage drop across the space charge region is orders of magnitude larger than that across the Helmholtz layer. Thus, the model predicts in particular that the electrical transient is virtually insensitive to the charge transfer reaction at the semiconductor/electrolyte interface. The electrical response to a ps laser pulse has already been analyzed in some detail before.[5] In the early ps time window the rise of the electrical transient is controlled by minority carrier diffusion. Corresponding experimental transients will be shown below for the n-Si electrode. In the ideal system the decay is exponential with time constant $C_S(R_M + R)$. In nonideal systems the decay can be strongly modified by recombination and detrapping events, if the latter occur in the same time window as the *RC*-controlled decay.

The behavior of the above model system has not been discussed yet for excitation with a rectangular light pulse in the μs−ms time range, the most commonly used excitation pulse for the investigation of photo-electrochemical systems. The prediction of the model is shown in Figure 2 for three different speeds of the interfacial discharge reaction of the photogenerated minority carriers. These simulated curves addressed a fictitious ideal system without recombination, where the current $j_S(t)$ followed directly the excitation profile $g(t)$. The following expressions were used for the two currents and the density of excess holes $p_S(t)$, respectively, at the semiconductor/electrolyte interface:

$$j_S(t) = qg(t) \tag{2a}$$

$$j_H(t) = qk_h p_S(t) \tag{2b}$$

$$dp_S(t)/dt = -k_h p_S(t) + g(t) \tag{2c}$$

Since time-resolved signals are measured and interpreted here, the concentration p_S is defined as surface density with the dimension cm^{-2} and the rate constant k_h as reciprocal time constant with dimension s^{-1}. These are the simplest rate equations describing the current flow in a photo-electrochemical cell under illumination. More elaborate cases will be discussed along with the experimental results. The simulations in Figure 2 differ only in the magnitude of k_h, the rate constant for hole transport across the Helmholtz layer. Three curves are shown for each case corresponding to fast, medium fast, and infinitely slow interfacial electron transfer: the voltage across the space charge layer $U_S(t)$, the voltage across the Helmholtz layer $U_H(t)$, and the voltage across the external resistor $U_M(t)$. The *RC* response occurred in the ns time regime. It was not time-resolved in the signals shown in Figure 2. Thus, the signal $U_M(t)$ is proportional to the photocurrent in the external circuit. It should be noted that the same signal would correspond to a photovoltage in a time window shorter than the *RC* constant.[5] In the actual experiments, the electrical transient was measured virtually in the absence of an external measuring resistance R_M. Since the current must be identical everywhere in the external circuit, we can translate the measured signals to the photocurrent by dividing the measured voltage by R_M, where R_M represents the total series resistance. The ratio C_H/C_S was assumed to lie in the range of 100. The simulations for the case of the fast reaction with $k_h = 10^8$ s^{-1} are shown at the top of Figure 2. In this case all three voltages $U_M(t)$, $U_S(t)$, and $U_H(t)$ followed directly the excitation profile $g(t)$. Due to the fast reaction, the magnitude of the last voltage was much smaller than the two others. By Kirchhoff's rules, the sum over all three voltages must add up to 0. In this case of the fast interfacial reaction the signal $U_M(t)$ indicates the true Faradaic current passing through the Helmholtz layer at the surface of the semiconductor electrode.

The case of a slower interfacial reaction with $k_h = 3 \times 10^3$ s^{-1} is shown in the middle of Figure 2. When the light was switched on, the current across the semiconductor initially charged C_S to same voltage $U_S(t)$ as in the above case. Virtually the same magnitude of the voltage was obtained for $U_M(t)$ at the external resistor. It should be noted that the signal $U_M(t)$ showed neither a rise time nor a decay time that could be related to the rate constant of the interfacial reaction k_h. Due to the large capacitor C_H, the signal $U_M(t)$ was controlled by the displacement current, i.e. by holes crossing the depletion layer as current flow $j_S(t) = g(t)$. The slowness of the interfacial discharge reaction led to the accumulation of holes at the crystal surface. The countercharge, i.e. electrons, moved through the external circuit to the outer Helmholtz plane. With ongoing accumulation of holes at the crystal surface, a significant voltage drop developed across the Helmholtz layer. This process continued until the discharge of holes through the Helmholtz capacitor via the interfacial charge transfer reaction reached the same rate as the generation of holes. This stationary situation had not yet been reached in the curves shown in Figure 2. The rise and decay of $U_H(t)$ was controlled by the hole transfer rate constant k_h. The same process controlled the time behavior of the signal $U_S(t)$, which showed in addition the displacement current, of course with opposite sign of $U_M(t)$.

The case of complete absence of interfacial electron transfer, i.e. $k_h = 0$ is shown in the lower part of Figure 2. In this case only accumulation of holes at the crystal surface and the pure displacement current were controlling the voltage signals. It should be noted that the voltage response at the external resistor $U_M(t)$ was the same as in the above cases, as it was controlled by the displacement current. For $k_h = 0$ the fictitious simple model predicted an infinite rise of the voltages U_S and U_H under continuous illumination. Such a situation will of course not occur in a real system since the accumulation of charges will eventually open up recombination channels and enforce new channels for interfacial reactions.

The most important result shown in Figure 2 is the virtually identical shape and magnitude of the experimentally accessible signal $U_M(t)$, irrespective of the tremendous differences in the velocity k_h of the interfacial electron transfer reaction. Inspection of Figure 2 shows that this type of experiment, i.e.

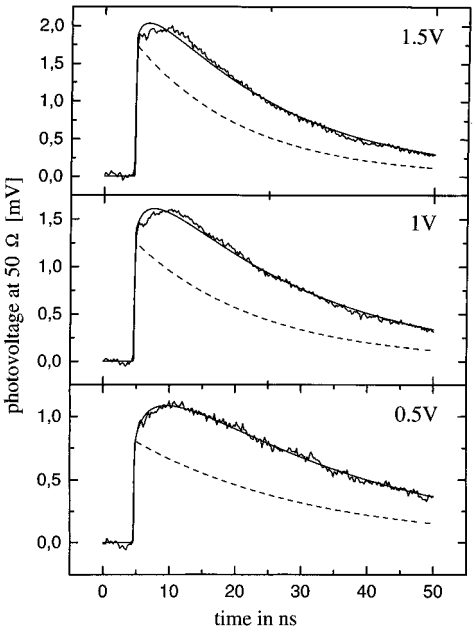

Figure 3. Experimental photocurrent transients and simulated transients (smooth curves) for ps light pulse excitation ($\lambda = 590$ nm, 10^7 photons/(mm^2 pulse)) of the n-Si/MeOH−$Me_2Fc^{+/0}$ cell at different bias. Redox electrolyte: 0.01 M 1,1′-dimethylferrocene, 0.01 M 1,1′-dimethylferrocenium tetrafluoroborate in a solution of 0.5 M LiCl in MeOH. Simulation parameters (solid curves): $k_h = 10^9$ s^{-1}, $k_q = 10^5$ cm/s, $D = 12$ cm^2/s, $\epsilon = 12$, $\tau = 1$ ms, $\alpha = 5 \times 10^3$ cm^{-1}, $N_D = 10^{15}$ cm^{-3}, $R_M = 50\ \Omega$, $C_H = 100$ nF, $C_S = 245$ pF (1.5 V band bending), 260 pF (1 V band bending), 510 pF (0.5 V band bending). Band bending is estimated from the experimentally determined flat-band situation as described in the text. The dashed curves were calculated with the same parameters by setting the minority carrier diffusion current to 0.

measurement of the signal $U_M(t)$ in the absence of a recombination reaction, does not yield information on the rate constant k_h of the interfacial charge transfer reaction. The identical conclusion had been reached already before[5] when modeling the signal $U_M(t)$ for the ps−ns time window. However, it will be shown below, by modeling the electrical response of a real system where recombination losses can occur, that the same measurement is extremely useful for exposing and monitoring recombination losses occurring in the ms time window in a real system. Such slow recombination events are occurring in virtually every experimental system firstly when the bands move closer to the flat band situation, secondly at high light intensity, and thirdly for a slow discharge reaction that leads to the accumulation of charge at the crystal surface. As will be shown in the next section, in a real photo-electrochemical system prepared with a neat single-crystal electrode, the signal $U_M(t)$ is most useful for monitoring charge carrier diffusion in the ps−ns window and recombination losses in the μs−ms window.

Modeling of Experimental $U_M(t)$ Transients

(a) Response in ps−ns Windows to a ps Light Pulse. The electrical response $U_M(t)$ of a semiconductor junction in the ps−ns window to a ps laser pulse is controlled by three processes: firstly, the diffusion of minority carriers created outside of the depletion layer,[5,8] secondly, the *RC* response,[5−7] and thirdly in specific cases also by fast recombination losses.[9] The latter process is absent, for example, in high-quality single-crystal Si-electrodes.

Figure 3 shows the experimental transient electrical response $U_M(t)$ of the n-Si/MeOH−$Me_2Fc^{+/0}$ cell with 0.5 M LiCl supporting electrolyte for three different values of the bias voltage along with the simulated model response. The bias is given as the experimental band bending V with respect to the two-electrode equilibrium situation. The signals were measured under a light flux of 10^7 photons/mm^2 per light pulse. At light fluxes exceeding 10^8 photons/mm^2 per light pulse, the rise and, even more so, the decay of the signal became increasingly slower. Also the general shape of the curves changed with the duration of the signal reaching 1 μs at 10^9 photons/mm^2 per light pulse. In the latter range of light intensity the number of photogenerated charge carriers approached the number of fixed donor charges in the space charge region. Therefore, these effects were attributed to the breakdown of the space charge field. For the signals shown in Figure 2 such effects can be ignored. The rise of the photovoltage signal consisted of two parts: The fast part rose as the apparatus function (100 ps), and the slow part rose over several ns. Separation of electron−hole pairs created within the space charge region occurred via a drift mechanism on a ps to sub-ps time scale. Min et al.[15] measured a transit time < 500 fs by using an electro-optic sampling technique at a GaAs electrode. The slower rise in the signals shown in Figure 2 was assigned to the diffusion of electron−hole pairs created outside of the space charge region. Such electron−hole pairs must perform a diffusional motion before they can enter the space charge field where they are separated, thus leading to the delayed rise of the photovoltage. In the Si samples, with $N_d \approx 10^{15}$ cm^{-3}, light at $\lambda = 590$ nm led to a diffusional component that contributed about one-third of the total photovoltage. This diffusional part of the signal was modeled with a time-dependent version of the Gärtner model.[16] This model had been successfully applied already for modeling the rising portion of the transient photovoltage in GaAs.[8] With the solution of the one-dimensional diffusion equation, the current flow in the semiconductor $j_S(t)$ can be written (drift and diffusion component) as follows:

$$\frac{j_S(t)}{q} = g(t) = g_0\left((1 - e^{-\alpha W})\phi(t) + e^{-\alpha W}\frac{k_q \alpha}{k_q/\sqrt{D} - \alpha\sqrt{D}} \times \int_0^t \phi(t - t')e^{-t'/\tau}\left(\frac{k_q}{\sqrt{D}} f\left(\frac{k_q}{\sqrt{D}}\sqrt{t'}\right) - \alpha\sqrt{D} f(\alpha\sqrt{D t'})\right) dt'\right) \quad (3)$$

$$f(z) = e^{z^2}\mathrm{erfc}(z)$$

where $\phi(t)$ is the normalized ($\int \phi(t)\, dt = 1$) excitation pulse time profile, W is the width of the space charge region, D is the hole diffusion constant, α is the absorption coefficient, τ is the minority carrier lifetime, g_0 is the number of photons/pulse, and k_q is an artificial boundary condition, which describes the velocity of the electron−hole pair separation at the boundary between the space charge region and the semiconductor bulk (see also Figure 1). A Gaussian pulse profile of 100 ps fwhmh was used for $\phi(t)$ to simulate the laser pulse and broadening due to the apparative response. The bias-dependent width of the space charge region W and the depletion layer capacitance C_S were modeled with Schottky's depletion layer approximation,[17]

$$W = \sqrt{\frac{2\epsilon\epsilon_0}{qN_D}(\phi_B + V_{ext})} \quad (4)$$

$$C_S = \frac{\epsilon\epsilon_0}{W} A \text{ [F]}$$

where ϵ_0 is the permittivity in vacuum, ϵ is the dielectric constant, N_D is the doping density, A is the electrode area, ϕ_B is the equilibrium band bending, and V_{ext} is the applied bias. Equations 1−4 represent a simple model that can describe the transient photocurrent in an "ideal" electrochemical or solid state photovoltaic cell with applied bias. Because all material-dependent parameters are well-known for Si, it could be checked whether the model was sufficient to describe the behavior of such a device. The smooth solid curves in Figure 3 show the result of a least-squares fit of the model to the experimental data. All parameters except C_S and g_0 were held constant for the fit. Although W was calculated from eq 4, C_S had to be fitted separately to obtain the best fits. The parameter k_q was found to be uncritical, as long as its value was high enough ($k_q > 10^5$ cm/s). The fit to the data was not perfect (Figure 3), but it has to be considered satisfactory, considering the simple model that was applied. The dashed curves in Figure 3 show simulations where the diffusion component was neglected. The only feature of these transients was the exponential decay with time constant $\tau = RC_S$. With decreasing band bending the depletion layer became shorter, C_S larger, and thus the RC decay time longer, as was expected from eq 4. It was clearly impossible to fit the model to the experimental data when the diffusion component was neglected. Kenyon et al.[7] performed similar experiments on the n-Si/MeOH−$Me_2Fc^{+/0}$ system, but with time resolution in the μs range. Therefore, the slow rise of the photovoltage due to the diffusional part in the photocurrent signal was not time-resolved in the signals reported by these authors. Consequently, a simple equivalent circuit without an active current source was sufficient to describe the observed exponential RC decay seen in their signals. Incorporation of the actual time dependence of the minority carrier motion as a property of an active current source as in the present model allows for an improved description of the system's behavior. The fits shown in Figure 2 of this paper and those shown in refs 8 and 9 clearly prove that modeling the system's behavior in the ps−ns window by introducing differential equations describing the motion and kinetics of the charge carriers represents a more powerful and physically meaningful approach than modeling the system's behavior with an equivalent circuit consisting of only passive elements.[2,4,7] This will become even more evident below, where recombination losses are considered in the μs−ms window.

The bias dependence of transients such as those shown in Figure 3 can be further analyzed as follows. Integration of the transient over time gives the amount of separated charge. The latter quantity can be plotted against the applied bias. From this plot one can determine the potential at which the separation of the photogenerated charges does not occur any more in the depletion layer. This potential indicates zero electric field in the semiconductor electrode; that is, it is the definition of the flat-band potential. As will be shown below, trapping and recombination effects occur in neat single-crystal electrodes in the ms range (compare Figure 4 below). However, they do not disturb the fast transients of photogenerated charge carriers in such electrodes. The above procedure represents, therefore, a more direct way of determining the potential where the flat-band situation arises than the conventional stationary method for measuring the Mott−Schottky relationship. As in conventional Mott−Schottky plots, the inverse square of the space charge capacitance determined from the fit to the transients was plotted against the applied bias. Whereas in conventional stationary measurements the linear relationship between $1/C_S^2$ and U_{ext} was often observed only at sufficiently high reverse bias, the Mott−Schottky plot extracted from the photocurrent transients was linear up to 100 mV from the flat-band potential. The intercept of the straight line with the U-axis gave the flat-band potential at −0.95 V with respect to the equilibrium potential of the system, which is controlled by the redox potential. This value implies a barrier height of ∼1.2 V. This value is even higher than had been obtained by surface conductance measurements on the same system.[18] It strongly supports the notion of a strong inversion layer at the n-Si/MeOH−$Me_2Fc^{+/0}$ interface. The uncorrected experimental barrier height of 1.2 eV is not consistent with the band gap of 1.1 eV. Considering the nonideal behavior of the system (compare the β value derived below), it is not really surprising that some degree of inconsistency did arise in the numerical values compared to an ideal system.

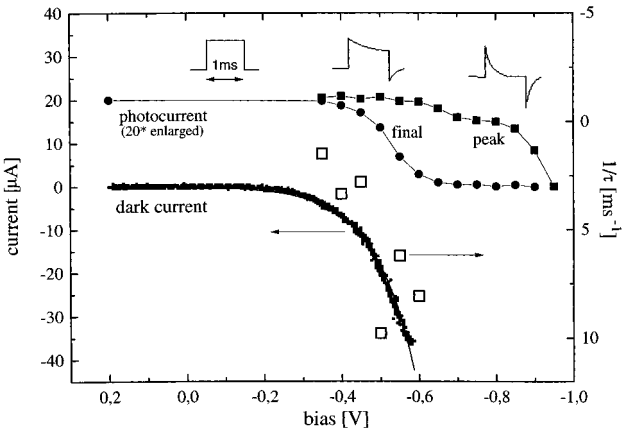

Figure 4. Summary of stationary and transient electrical signals measured at the n-Si/MeOH−$Me_2Fc^{+/0}$ cell. Redox electrolyte: 0.005 M 1,1′-dimethylferrocene, 0.005 M 1,1′-dimethylferrocenium tetrafluoroborate in a solution of 0.5 M LiCl in MeOH. The squares and dots represent characteristic parts of the photocurrent transients measured under rectangular light pulse excitation (see text). The transients occurring in the corresponding bias range are shown in the upper part of the figure.

(b) Response in μs−ms Time Windows to a Rectangular Light Pulse. Figure 4 gives a summary of stationary and time resolved U_M signals measured at the n-Si/$Me_2Fe^{+/0}$−MeOH system. Firstly, the dark current was measured. Afterward, a series of time-resolved photocurrent signals were measured at different values of the bias voltage. The light intensity was 0.2 mW/cm^2 at $\lambda = 655$ nm. The shape of the transients is depicted in the upper part of Figure 4. At high reverse bias, > -0.4 V, the photocurrent followed directly the rectangular intensity profile of the excitation light. The rise time of the signal was limited by the bandwidth of our current amplifier (300 ns). At potentials < -0.4 V the initial photocurrent decayed to a lower stationary value. With decreasing band bending (more negative potentials), the decay time became shorter and the magnitude of the stationary photocurrent smaller. The initial photocurrent disappeared at potentials < -0.9 V. When the light was switched off, the current returned to the value of the dark current with the same time constant that controlled the decay of the photocurrent. In Figure 4 the initial amplitude ("peak") of the photocurrent transients is shown as solid squares and the stationary photocurrent is shown as solid spheres. The latter agreed with the stationary measurement. The peak photocurrent showed only a small decrease at potentials > -0.8 V. At −0.9 V the decay time was 2 μs and the amplitude was also reduced due to bandwidth limitations of the potentiostat. The stationary photocurrent disappeared at a much more positive potential than the "peak" photocurrent. The breakdown potential for the "peak" photocurrent measured in the ms window agreed well with the breakdown potential

for the peak photocurrent measured in the ns window, the latter in response to excitation with a ps light pulse. Thus, with a moderate time resolution of 1 μs, the potential for the flat-band situation was determined with the same precision as in the measurement with ps resolution. The decay of the photocurrent was exponential. The bias dependence of the decay rate $1/\tau$, time constant τ, also followed an exponential law (Figure 4, empty squares). For this bias dependence of $1/\tau$ the coefficient in the exponent was about 10, with slight variations between different samples. The photocurrent transients were found to depend only slightly, and in a nonsystematic way, on the concentration of the redox species in solution. Lewis et al. reported that the dark current remained independent of the concentration of the oxidized species;[19] this was also confirmed here.

The behavior of the transient photocurrent as described above appears to be quite common in the photo-electrochemistry of semiconductors. It has often been observed in cyclic voltammetry experiments, where the sample was illuminated with chopped light during the scan.[20−23] Since a comparable behavior has not been reported for solid state photovoltaic cells, the question arises whether the decay of the initial photocurrent is an intrinsic property of the semiconductor−electrolyte interface, most likely due to the fairly long lifetime of the charge carriers at the crystal surface. To our knowledge Peter[24] was the first in suggesting a model that could explain the time-dependent decay of photocurrent transients as in Figure 4. His transients were measured at p-GaP, and the decay of the photocurrent was ascribed to a recombination current via "near" surface states. The term "near surface states" was introduced since the latter were assumed to equilibrate with the bulk of the semiconductor and not with the redox system. It was suggested that the shift in the onset of the stationary photocurrent observed at higher light intensities could be related to this recombination current. Accumulation of holes near the surface can explain the difference between the onset bias for the "peak" and stationary magnitude of the photocurrent in Figure 4. A change in band bending under illumination was not considered in Peter's model. In essence, Peter's surface recombination current can be viewed as increased (compared to the dark situation) majority carrier current. At the semiconductor surface there is a sink for the majority carriers, electron transfer from redox ions. Opening of a second reaction path, i.e. recombination via surface states, can increase the net flow of majority carriers, and the total current will change under illumination. In the present experiments minority carriers, i.e. holes in n-Si, were efficiently collected as long as the voltage drop was kept > 100 mV with respect to the flat-band situation, as can be seen from the peak photocurrent in Figure 4. The decay of the photocurrent must be due to the accumulation of charge carriers at or near the interface.

The basic mechanism of such a recombination effect can be illustrated with the simplest case of direct recombination between electrons and holes, as illustrated in Figure 1. It is clear that this is not likely to be the dominant recombination path in Si with an indirect band gap. The simplest equations for the direct recombination case are as follows:

$$j_S(t) = q(g(t) - k_r n_S p_S(t)) \tag{5a}$$

$$j_H(t) = q k_h p_S(t) \tag{5b}$$

$$dp_S(t)/dt = -(k_h + k_r n_S) p_S(t) + g(t) \tag{5c}$$

where n_S = majority concentration in the dark and p_S = additional minorities due to illumination. Equation 5a describes

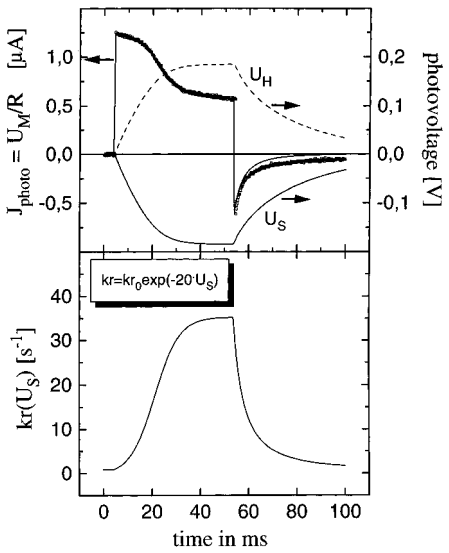

Figure 5. Experimental and simulated transient photocurrent of a n-Si photo-electrochemical cell in the absence of a redox couple (redox electrolyte consisted of 0.5 M LiCl in MeOH). Other experimental conditions were identical with the measurement shown in Figure 4.

only recombination events that occur in addition to the dark situation. The change in the majority carrier current under illumination is $-qk_r n_S p_S(t)$. To keep the model as simple as possible, n_S was assumed to stay constant under illumination with no change in band bending. This simple model already gave the shape of the transients shown in Figure 4. The change with bias occurred due to the Boltzmann-dependent change of n_S with the $k_r n_S \approx \exp(-qU/(k_B T)) = \exp(-U\beta)$, with U being the applied bias. The exponential dependence of this rate constant on U was confirmed indeed by the fit, but with the coefficient $\beta = 15\ V^{-1}$ and not with $\beta = 40$, as would be expected from the Boltzmann relationship. The latter corresponds to the ideal diode quality factor. The dark current, measured in a bias range without mass transport limitation of the redox ion concentration, also gave the factor $\beta = 20\ V^{-1}$ for the exponential bias dependence. Thus, it was found that the bias dependence for the time constant derived from the shape of the photocurrent transients was clearly linked to the experimental bias dependence of the dark current (Figure 4), both with approximately the same coefficient, deviating strongly from that of the ideal diode equation. It was checked that complications that can arise at high light intensities did not affect this result. Such complications were observed to set in at much higher light intensities and brought about drastic changes in the shape of the photocurrent transients. Such high light intensity effects will not be discussed in this paper.

Further experiments were carried out showing that the recombination effects seen in the transients of Figure 4 cannot be ascribed to the severe accumulation of the holes at the crystal surface. The latter situation is expected to arise for a very slow discharge reaction at the interface. This slow reaction case was investigated at the same light intensity as employed for the signals shown in Figure 4 but in the absence of the redox ions in the solution. The ensuing shape of the transient is shown in Figure 5. The occurrence of the photocurrent proved that there was an initial band bending in the dark that was ascribed to equilibration of Bardeen-type surface states[25] with the electrons in the bulk. The transient is shown as a noisy curve in the upper graph of Figure 5. It was recorded with the cell biased to +0.4 V. The shape of the transient in Figure 5 is obviously very different from that shown in Figure 4. As predicted by the model simulation shown in Figure 2, a fast rise of the initial

photocurrent was observed (Figure 5) even in the virtual absence of discharge reactions across the Helmholtz layer. The signal was nonsymmetric with respect to switching on and off the light. Lowering the light intensity by a factor of 10 removed the conspicuous S-shaped dip in the transient, with only the slow decay, seen initially in the transient in Figure 5, remaining throughout the duration of the light pulse. The other curves shown in Figure 5 are simulations applying eq 5. The agreement between the simple model and the experimental signal is remarkable. In Figure 5 only a minor deviation can be seen of the simulation from the experimental transient in the dark period after the light is switched off. In this simulation, the recombination term was coupled to the voltage U_S that increased across the space charge capacitor due to massive accumulation of photogenerated charge in the semiconductor, i.e. $k_R = kr_0 \exp(-\beta U_S)$. The time evolution of this recombination term is shown in the lower graph in Figure 5. The space charge capacitance was assumed to be independent of U_S. This assumption appeared justified by the much shorter time scale, i.e. ns, for the *RC* response. From the fit of the model to the data, the rate constant for the hole discharge was found to be extremely small, $k_h = 31\ s^{-1}$, as was expected for the absence of redox ions. At $U_S = 0$ the recombination rate was $k_R = 0.9\ s^{-1}$. The simulation depended critically on the experimental factor β. As in the fits described above, the best fit gave again $\beta = 20\ V^{-1}$, i.e. the value found in the bias dependence of the dark current.

Discussion

Figure 1 gives the simplified model,[5] where the spatial separation of photogenerated electrons and holes is described with an equivalent circuit, with the capacitance C_S standing for the charge separation across the depletion layer in the semiconductor, and the capacitance C_H for charge separation across the Helmholtz layer at the surface of the semiconductor. Gottesfeld et al.,[2] Wilson et al.,[4] and Lewis et al.[7] have confirmed the usefulness of this approximation with respect to the *RC* behavior of the system. As pointed out before,[5,8,9] the important physical processes occurring in this system, e.g. time-dependent diffusion of the minority carriers toward the depletion layer (Figure 3), and recombination of electron−hole pairs across the depletion layer (Figures 4 and 5) cannot be modeled with an equivalent circuit consisting only of passive circuit elements. In the simplest acceptable kinetic model the description of these processes requires the use of differential equations describing these processes as properties of active current sources (e.g. eqs 2, 3, and 5) embedded into the equivalent circuit (eq 1). The influence of charge carrier kinetics on the shape of electrical transients in response to a ps light pulse was described before in some detail for time windows shorter than the *RC* response,[5,8] typically over some ns. As an experimental example the diffusion of minority carriers was shown to control the rise of the photovoltage in a n-GaAs electrode.[8] The corresponding diffusion-controlled rise in the photovoltage is shown in Figure 3 of this paper for the minority carriers in n-Si. Since the lifetime of the minorities is much longer in n-Si than in GaAs, the diffusion-controlled rise of the photovoltage could be measured over a much longer period of time in the present system. The theoretical model gave a satisfactory fit to the experimental transients recorded at different bias voltages at the n-Si electrode (Figure 3). As will be shown elsewhere, the *RC* constants determined from the fit to the decay behavior of the transients at different bias voltages allow for the construction of a Mott−Schottky type plot, $1/C^2$ versus bias voltage, that remains linear up to a 100 mV approach of the flat-band situation. This experimental method for determining the flat-band potential appears to be superior to measuring conventional stationary Mott−Schottky plots at different frequencies. The method gives also the voltage difference between the flat-band situation and the equilibrium situation in the system, thereby showing the position of the Fermi level in the dark with respect to the band edges of the semiconductor.

The central point in the present paper is the application of the model illustrated in Figure 1 to the electrical response obtained with rectangular light pulses in the ms time domain (Figures 2, 4, and 5). The first important result is the prediction that the photocurrent transient, $I_M(t) = U_M(t)/R_M$, measured at the external resistor R_M (Figure 1) is independent of the magnitude of the rate constant for the interfacial discharge of the photogenerated charges in the absence of a competing recombination reaction (transients in Figure 2 and the initial magnitude of the transients in Figures 4 and 5). This inability to distinguish also with ms transients between the displacement current and the true Faradaic current has been frequently overlooked in the discussion of such slow transient signals. This particular prediction of the model might suggest at first glance that measurements of electrical transients in response to a rectangular light pulse in the ms range will not offer much useful information concerning the semiconductor/electrolyte system. However, the contrary is demonstrated since the transients are a sensitive probe for recombination losses. This was seen in the changed shape of such transients due to the occurrence of recombination when the applied bias voltage was changed (Figure 4) and when the speed of the interfacial discharge reaction for the minority carriers was changed (Figure 5). The recombination rate constants obtained from modeling the photocurrent transients at low photon flux followed the same bias dependence as the stationary forward dark current (Figure 4). The identical bias dependence was determined from the change in photovoltage when minority carriers were accumulated at one side of the space charge layer. The extremely slow discharge into the electrolyte was achieved in the absence of suitable redox ions in the contact solution (Figure 5). It was shown in both cases that there was a close relationship between the bias dependence of the recombination losses seen in the photogenerated electrical response and the bias dependence of the forward dark current (Figure 4). A realistic physical model for the mechanisms that control the recombination losses thus requires the full understanding of the current−voltage curve in the dark, i.e. in the present case for the interface with an inversion layer. To our knowledge this latter case has not been analyzed, and this task is left here for a future contribution. Finally a remark appears in order concerning specific electrochemical recombination channels that can open up in the present system at a high photon flux, e.g. when the redox ions are consumed in the interfacial reactions at high turnover. In this case the discharge reaction via one of the bands, e.g. transfer of holes from the valence band to reduced redox ions at the crystal surface, can change the concentration of the thus produced oxidized redox ions at the surface. This in turn can lead to an enhanced current flow via the conduction band due to the now higher concentration of oxidized redox ions with the electrons in the conduction band. Thus, a specific electrochemical short circuit path can be established at high photon flux at this electrochemical interface in addition to the recombination paths in the semiconductor. This electrochemical short circuit is illustrated in Figure 6c. It should not arise when an ideal Schottky interface is formed between a semiconductor and a metal, or metal/oxide contact layer. In the latter cases the density of occupied and nonoccupied electronic states can

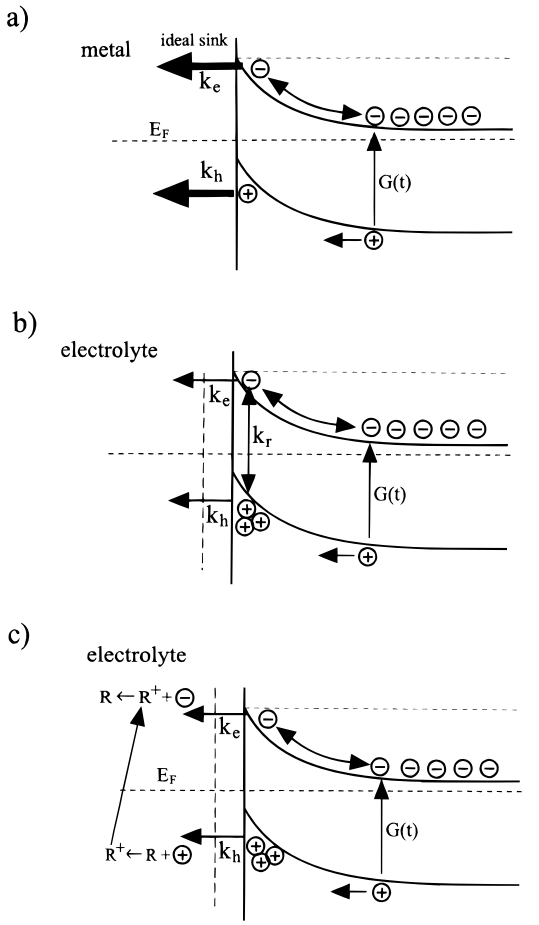

Figure 6. Illustrations of charge carrier kinetics at the n-semiconductor interface under light excitation for a metal contact (a) and an electrolyte contact (b and c). At the semiconductor/electrolyte interface, the slow discharge of photogenerated holes leads to recombination near the surface (b), and for strong accumulation to an electrochemical short circuit in the electrolyte at the interface (c).

be assumed to stay constant in the metal, irrespective of the magnitude of the interfacial current flow (Figure 6a). The case analyzed in this paper is illustrated in (Figure 6b). Recombination losses occurring in the semiconductor at low light intensity were detected and analyzed by fitting the change in the shape of photocurrent transients in μs−ms windows. The situation for moderately fast charge carrier discharge across the Helmholtz layer led to moderate accumulation of minority carriers at the interface (Figure 4). The recombination losses were found to accelerate and drastically change the shape of the transient for longer light pulses when the interfacial discharge reaction was extremely slow and charge carrier accumulation led to strong band bending under the light (Figure 5).

References and Notes

(1) Gerischer, H. In *Photovoltaic and Photoelectrochemical Solar Energy Conversion*; Cardon, F., Gomes, W. P., Dekeyser, W., Eds.; Plenum Press: New York, 1981; p 199.
(2) Harizon, Z.; Croitoru, N.; Gottesfeld, S. *J. Electrochem. Soc.* **1981**, *128*, 551−554.
(3) Willig, F.; Bitterling, K.; Charle, K. P.; Decker, F. *Ber. Bunsen-Ges. Phys. Chem.* **1984**, *88*, 374−378.
(4) Wilson, R. H.; Sakata, T.; Kawai, T.; Hashimoto, K. *J. Electrochem. Soc.* **1985**, *132*, 1082−1087.
(5) Willig, F. *Ber. Bunsen-Ges. Phys. Chem.* **1988**, *92*, 1312−1319.
(6) Gottesfeld, S. *Ber. Bunsen-Ges. Phys. Chem.* **1987**, *91*, 362−369.
(7) Kenyon, C. N.; Ryba, G. N.; Lewis, N. *J. Phys. Chem.* **1993**, *97*, 12928−12936.
(8) Bitterling, K.; Willig, F. *J. Electroanal. Chem.* **1986**, *204*, 211−224.
(9) Bitterling, K.; Willig, F.; Decker, F. *J. Electroanal. Chem.* **1987**, *228*, 29−44.
(10) Byrne, G. D.; Hindsmarsh, A. C. *J. Comput. Phys.* **1987**, *70*, 1−62.
(11) Dennis, J. E.; Gay, D. M.; Welsch, R. E. *ACM Trans. Math. Softw.* **1981**, *7*, 369−383.
(12) Sze, S. M. *Physics of Semiconductor Devices*, 2nd ed.; John Wiley & Sons: New York, 1981.
(13) Bard, A. J.; Faulkner, L. R. *Electrochemical Methods−Fundamentals and Applications*, 1st ed.; John Wiley & Sons, Inc.: New York, 1980.
(14) Levich, V. G. *Adv. Electrochem. Electrochem. Eng.* **1966**, *4*, 249−371.
(15) Min, L.; Miller, R. J. D. *Appl. Phys. Lett.* **1990**, *56*, 524−526.
(16) Gärtner, W. W. *Phys. Rev.* **1959**, *116*, 84−87.
(17) Schottky, W. *Z. Phys.* **1942**, *118*, 539.
(18) Laibinis, P. E.; Stanton, C. E.; Lewis, N. S. *J. Phys. Chem.* **1994**, *98*, 8765−8774.
(19) Kumar, A.; Lewis, S. *J. Phys. Chem.* **1991**, *95*, 7021−7028.
(20) White, H. S.; Fan, F. F.; Bard, A. J. *J. Electrochem. Soc.* **1981**, *128*, 1045−1055.
(21) Peat, R.; Riley, A.; Williams, D. E.; Peter, L. M. *J. Electrochem. Soc.* **1989**, *136*, 3352−3355.
(22) Li, J.; Peat, R.; Peter, L. M. *J. Electroanal. Chem.* **1984**, *165*, 41.
(23) Albery, W. J.; Bartlett, P. N. *J. Electrochem. Soc.* **1982**, *129*, 2254−2261.
(24) Peter, L. M.; Li, J.; Peat, R. *J. Electroanal. Chem.* **1984**, *165*, 29−40.
(25) Bardeen, J. *Phys. Rev.* **1947**, *71*, 717.